Novel antibacterial polyurethane and cellulose acetate mixed matrix membrane modified with functionalized TiO_2 nanoparticles for water treatment applications

Adnan Ahmad[a], Aneela Sabir[a], Sadia Sagar Iqbal[b*], Bassem F Felemban[c] , Tabinda Riaz[a], Ali Bahadar[d], Nazia Hossain[e*], Rafi Ullah Khan[a], Fawad Inam[f]

[a]Institute of Polymer and Textile Engineering and Technology, University of the Punjab, Quaid-e-Azam Campus, P.O. Box 54590, Lahore, Pakistan

[b]Department of Physics, The University of Lahore, P.O. Box 54000, Lahore, Pakistan

[c]Department of Mechanical Engineering, College of Engineering, Taif University, P.O. Box 11099, Taif 21955, Saudi Arabia

[d]Department of Chemical and Materials Engineering, King Abdulaziz University, Rabigh 21911, Saudi Arabia

[e]School of Engineering, RMIT University, Melbourne VIC 3001, Australia

[f]School of Architecture, Computing and Engineering, University of East London, Docklands campus, E16 2RD, London, United Kingdom

[*]Corresponding author at: Tel.: +61 480123691; E-mail address:bristy808.nh@gmail.com (Nazia Hossain); School of Engineering, RMIT University, 128 La Trobe Street, Melbourne, VIC 3001, Australia; Email address: sadiasagariqbal.pu@gmail.com (Sadia Sagar Iqbal), Department of Physics, The University of Lahore, P.O.Box 54000, Lahore, Pakistan.

Abstract

Bacterial contamination is one of the leading causes of water pollution. Antibacterial polyurethane/cellulose acetate membranes modified by functionalized TiO_2 nanoparticles were processed and studied. TiO_2 nanoparticles were prepared and ultraviolet (UV) irradiated to activate their photocatalytic activity against *Escherichia coli* (*E. Coil)* and *Methicillin-resistant Staphylococcus aureus (MRSA)* bacteria. Functionalized TiO_2 nanoparticles were incorporated in flat-sheet mixed matrix membranes (MMMs). These membranes were characterized for their different properties such as morphology, thermal stability, mechanical strength, surface wettability, water retention, salt rejection, water flux, and their antibacterial performance against *E. Coil* and *MRSA* was also tested. The activity of nanoparticles against MRSA and *E. coli* was analyzed using three different concentrations, 0.5 wt%, 1.0 wt% and 1.5 wt% of nanoparticles and 0.5 wt% of TiO_2 nanoparticles showed maximum growth of bacteria. The maximum inhibition was observed in membranes with maximum nanoparticles when compared with other membranes. All these characteristics were strongly affected by increasing the concentration of TiO_2 nanoparticles in the prepared membranes and the duration of their UV exposure. Hence, it was proved from this analysis that these TiO_2 modified membranes exhibit substantial antibacterial properties. The results are supporting the utilization of these materials for water purification purposes.

Keywords: PU/CA membrane; reverse osmosis; TiO_2 nanoparticles; water desalination; antibacterial;

1. Introduction

Water is the basic necessity of life. By 2025, three billion people are anticipated to face severe water scarcity, described as the single greatest threat to health, the environment, and global food security (Hossain and Mahmud, 2019). Different causalities because of water-borne diseases like dysentery, diarrhea, gastroenteritis, and nausea increase daily. Microbial contamination of water is a severe threat to public health and must be treated to decrease casualties. Water treatment and water recycling will thus play a steadily increasing role, with membrane technology constantly gaining market share, applying from small to large scales, and retaining compounds with various sizes. It has some inherent advantages, such as porosity, pore size, and hydrophilicity (Kumar et al., 2013; Halder et al., 2020).

Novel high-performance polymeric membrane materials have gained much attention over the last few decades for different industrial and commercial applications (Geise et al., 2010). The membrane separation technique is closely related to its synthesis and material selectivity concerning its usage (Vassolo and Döll, 2005). There are numerous membrane processes for the separation of the materials which depend upon pore size and diffusion through the membrane, like microfiltration (MF), ultrafiltration (UF), reverse osmosis (RO), and electro-dialysis (ED) (Shannon et al., 2010). These processes are used individually or with the traditional methods for different industrial applications such as the food and beverage industry, pharmaceutical, paper, textile industry, mineral processing, mining, battery, and many other industries. Another significant usage of the membrane is binders for recycling rare metals, removing heavy metal ions from industrial effluents (Water and Organization, 2004; Shannon et al., 2010). The chemical processing industries are groomed with synthetic polymeric membranes in their physicochemical properties, such as thermo-mechanical stability and resistance to pH in different solvents. For industrial effluents, recovery of some valuable constituents is essential, so different filtration

processes are used to separate those materials. Ultrafiltration and reverse osmosis are the most feasible techniques used for filtration on an industrial scale due to their low maintenance and running cost, high permeation, and attractive salt rejection (Organization, 1993). There are several polymers available for the synthesis of the membranes.

The selection of the desired polymer is based upon the membrane type and end application of the synthesized membrane. The most demanding polymers for the synthesis of a membrane are cellulose acetate (CA), polyurethane (PU), polysulfone (PS), polyvinyl pyrrolidone (PVP) and polyvinyldifloride (PVDF) (Nagaraju and Sastri, 1999; Shar et al., 2009; Majid et al., 2019). Among these polymers, cellulose acetate is well known for membrane manufacturing due to its low cost, superior film ability, attractive salt rejection, and hydrophilicity. Moreover, it possesses high fouling resistance and significant compatibility with other polymers for blending, but it has low mechanical strength and is susceptible to chlorine attack (Jacangelo et al., 1997; Azizullah et al., 2011; Ahmad et al., 2016; Majid et al., 2016). The blending of polymers is a very convenient way to manufacture different membranes for different applications. This technique allows to tailor of the characteristics of the end product and can enhance its performance and efficiency (Geise et al., 2010). The physicochemical behavior of the membranes can be improved by this blending technique (Ahmadiannamini et al., 2017). There are various other polymers available to synthesize the membranes concerning their end uses.

PU is the most widely used polymer in different industries due to its distinctive thermo-mechanical properties. Its high flexibility, tensile strength, and resistance to harsh conditions (temperature and pH) make it attractive for industrial usage (Gabriel et al., 2017; Ibrahim et al., 2017). PU is composed of soft segments (polyether-polyols or polyester-polyols) and hard segments (aromatic or aliphatic diisocyanates) in an alternating manner. PU membranes are mostly

heterogeneous, as the hard and soft segments are usually dispersed matrix form (Rahimpour et al., 2012; Ahmad et al., 2015).

Nevertheless, cellulose acetate-based membranes need modifications concerning hydrophilicity and hydrophobicity (Shannon et al., 2010). In the meantime, polyurethane possesses high porosity, low weight/volume ratio, appreciable abrasion, and oil resistance. Hence, it can be blended with cellulose acetate to get superior properties concerning thermo-mechanical behavior, flux, salt rejection.

The incorporation of tasks specific nanoparticles can further enhance the performance of polymeric membranes. TiO_2 nanoparticles are used as an additive to increase hydrophilicity, permeability, and antifouling properties of the membrane (Blake et al., 1999; Rahimpour et al., 2012; Yuzer et ali., 2022; Chen et al., 2020) . These nanoparticles are preferred because of their super-hydrophilic and photocatalytic effects. These nanoparticles can be used to inhibit bacteria by utilizing their photocatalytic behavior with UV light (Yan et al., 2013). Photocatalysis provides a hygienic environment for the water disinfection process (Ekey, 2013). The influence of TiO_2 particles in altering the membrane properties was studied by several researchers (Kwak et al., 2001; Li et al., 2007; Rahimpour et al., 2011; Arsuaga et al., 2013). In one of the previous studies, researchers have highlighted this photocatalytic effect of TiO_2 nanoparticles for antibacterial and antifouling properties of prepared membranes. These PVDF membranes were prepared using sulfonated polyethersulfone (SPU/CA), TiO_2 nanoparticles and polyvinylpyrrolidone (PVP) in the casting solution (Mingliang et al., 2011). The membrane showed good antibacterial results when exposed to UV light because of the photocatalytic property of TiO_2 nanoparticles. In another study, the antifouling properties of membranes were enhanced by adding TiO_2 nanoparticles into the sulfonated polyethersulfone mixed matrix membranes. The contact angle analysis indicated increased hydrophilicity of this membrane due to the addition of nanoparticles. It was also

observed that the membrane prevented its fouling from different substances (Bagheri et al., 2013; Abdullah et al., 2019). The functionalization of TiO_2 nanoparticles was done to avoid their agglomeration in the membrane, impart anti-fouling properties, and ensure the proper distribution of particles in the membrane.

Therefore, the present study aims to prepare antibacterial PU/CA membranes with hydrophilic nature capable of inhibiting bacterial activity current in the water. TiO2 nanoparticles were functionalized and incorporated in PU/CA mixed matrix membrane (MMMs) to achieve this objective. Synthesis, characterization, and antibacterial testing of TiO_2 nanoparticles were carried out. The functionalized TiO_2 nanoparticles were then incorporated into PU/CA MMMs. The prepared membranes were characterized for their antibacterial properties in addition to their morphology, surface wettability, water retention, salt rejection, flux, thermal and mechanical properties.

2. Materials and Methods

2.1 Materials

Titanium dioxide anatase (general purpose reagent) was obtained from DAEJUNG chemicals & metals Co. Ltd., Korea. Chloroform and (3-Aminopropyl) trimethoxysilane (APTMS) were acquired from Merck, Germany. Cellulose acetate (CA, M_w = 32,000), isophorone diisocyanate (IPDI) M_w = 222.28 g/mol, polyethylene glycol M_w = 3000 (PEG–3000), dibutyltin dilaurate (DBTL), ethylene glycol (EG) M_w = 62 g/mol, epichlorohydrin (ECH) and ethyl acetate (EA) were also supplied by Merck, Germany. *E. coli* gram-negative bacteria (ATTC25922), Methicillin-*Resistant StaphylococcusAreus* (*MRSA*), gram-positive bacteria (ATCC25923), *Mueller-Hinton*

Agar (MHA), yeast extract, and tryptone (TB medium) were also used. All of these chemicals were of analytical grade and were used without any further purification.

2.2.Synthesis of TiO_2 nanoparticles

The liquid impregnation method was used for the synthesis of TiO_2 nanoparticles. Titanium dioxide anatase (3 g) was added in 150 mL of deionized water and magnetically stirred at 400 rpm for 48 hours. The solution was then sonicated for 150 minutes. The solution was left for 12 hours to settle down at ambient temperature and then placed in a drying oven (LVO- 2040, Lab Tech, Korea) for 12 hours at 105 ºC. The calcination of the resultant material was carried out in the furnace at 400 ºC for 6 hours. Finally, TiO_2 nanoparticles in powder form were obtained.

2.2.1. Functionalization of TiO_2 nanoparticles

TiO_2 nanoparticles (2g) were added in 100 mL chloroform and sonicated for 30 minutes. After sonication, APTMS (6mL) was added to this solution and sonicated for another 5 hours to achieve better dispersion of nanoparticles. The solution was magnetically stirred for 1 hour at 70 ºC then centrifuged at 400 rpm for 30 minutes to remove excess solvent. The obtained residue was then oven-dried for 12 hours at 80ºC. FTIR later confirmed the presence of amine groups over the particle surface.

2.2. Preparation of chain extended polyurethane (PU)

An assembly containing a thermometer, nitrogen gas inlet, mechanical stirrer, 4 necked-flask (250 mL), condenser and rotamantle was used to synthesize polyurethane. Before injecting an ingredient into the flask, the flask was rinsed with the proposed solvent (ethyl acetate) and preheated at about 60-70ºC. According to the adjusted molar ratio of IPDI: PEG: EG (2:1:1) respectively, the chemicals were injected into the system systematically with nitrogen gas to remove oxygen from the reaction vessel. PEG was melted and poured into the reaction vessel with

catalyst (DBTL, 1 wt. % of PEG) for 10 minutes before the addition of IPDI. The predetermined amount of IPDI was added into the system by injection syringe followed by vigorous mechanical stirring. Stabilization of temperature is significant in this process, so a condenser was attached to the flask during the reaction. The process was exothermic, and the mechanical stirring had to be vigorous throughout the reaction till the addition of the chain extender. The addition of THF attained the controlled viscosity of the pre-polymer. The temperature was maintained at 80ºC and a clear transparent pre-polymer was obtained after 4 hours. According to the molar ratio of IPDI: PEG: EG (2:1:1) respectively, the –NCO contents were not utilized during the reaction. Ethylene glycol was added slowly to the reaction vessel, which acted as a chain extender for the synthesized pre-polymer. After the addition of EG, gentle stirring was provided for 30 minutes. Finally, the chain extended colorless PU was obtained and left in air-tight vials for 24 hours. After different time intervals, samples were collected for FTIR to check the completion of the reaction by identifying –NCO peaks.

2.3.Preparation of PU/CA blend membranes

A solution casting method was used to synthesize the Polyurethane (PU)/Cellulose acetate (CA) composite membranes. Firstly, the CA was dissolved in ethyl acetate with mild heating, and then PU was added to the solution. The temperature was kept constant at 70 ºC with mild stirring until a clear and homogeneous solution was observed after 4 hours. The prepared solution was poured on a glass plate and kept in the oven at 40 ºC. After 5 hours, the temperature was raised from 40 ºC to 75 ºC. After 10 hours, a transparent membrane was obtained and peeled off the petri plate using a sharp blade. The blend membranes were prepared in four different ratios of PU and CA. The percentages for PU/CA blend were 90/10, 80/20, 70/30 and 60/40 named PC-1, PC-2, PC-3, and PC-4, respectively. The thickness of all PU/CA membranes was in the range of 35-40 μm. The obtained blend membranes were clear and transparent in appearance. PC-2 membrane

was selected for further modification due to better permeation properties as mentioned in Table 3. The results showed the optimum values of Flux and salt rejection for PC-2. In PC-1 the salt rejection is compromised but flux value is high, and vice versa in PC-3 and PC-4 membrane.

2.4.Titania modified membranes

PC-2 membrane was modified by adding TiO_2 in five different concentrations, i.e., 0.5%, 0.75%, 1.0%, 1.25%, and 1.50% weight percent respectively, into the polymer solution of PU/CA and ethyl acetate. The obtained solutions were then magnetically stirred for 3 hours at 55 ºC to obtain homogeneous solutions. These solutions were magnetically stirred overnight at room temperature. Then the membrane was prepared using a thin film applicator and custom design tray by solution casting and solvent evaporation technique. The casted membrane was immersed in distilled water for precipitation and removal of solvent. Eventually, air drying was done under ambient conditions to obtain modified blend membranes.

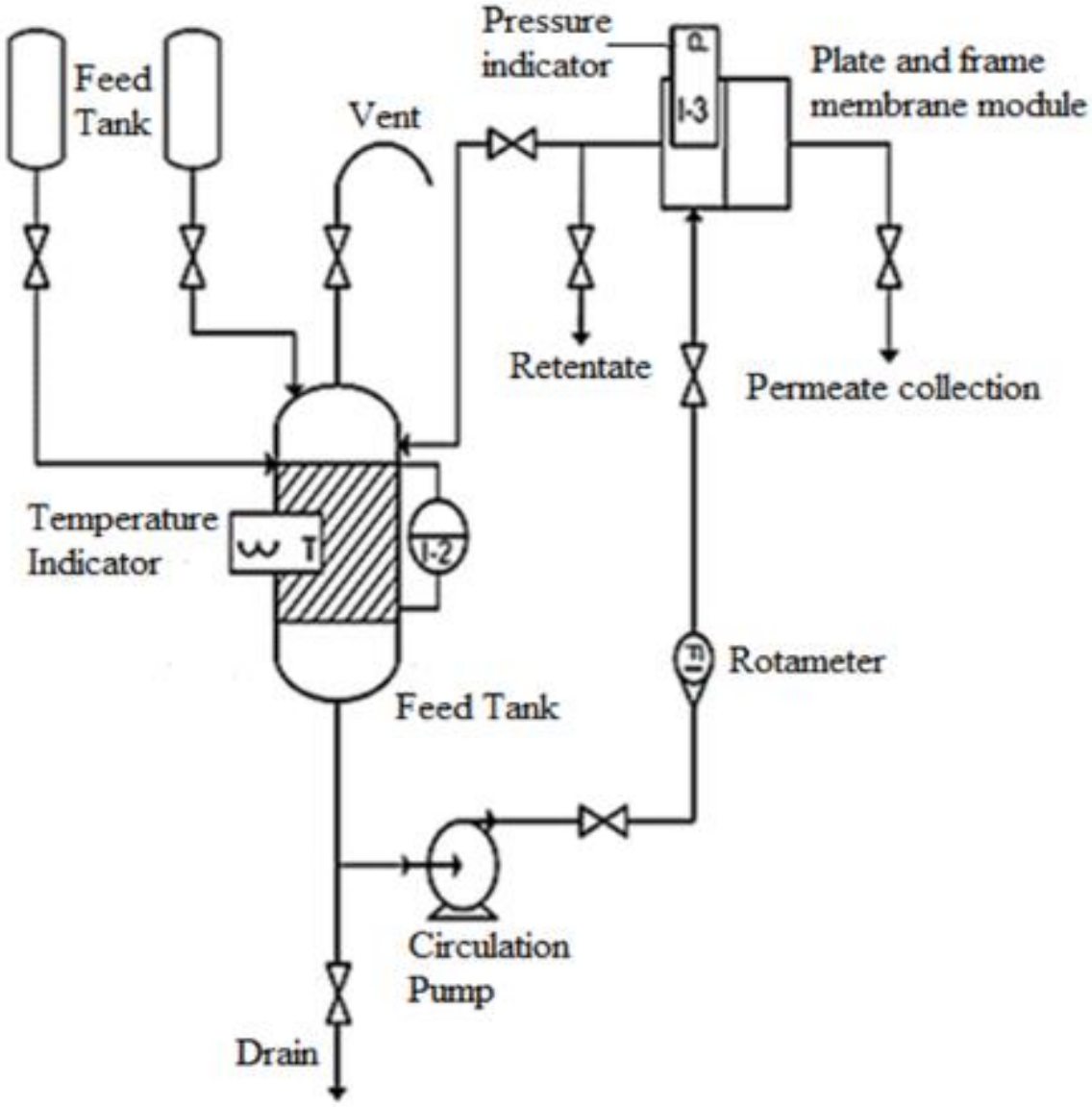

Figure. 1. Indigenously fabricated lab scale RO plant

2.5.Characterizations

2.5.1. FTIR

Fourier transform infrared spectroscopy (FTIR; Perkin Elmer FTIR 100 Spectrometer,) was performed before and after functionalization of particles. This was to confirm the presence of silane moiety and fabricated TiO_2 nanoparticles in reinforced PU/CA membranes.

2.5.2. XRD

The X-Ray diffraction (XRD; STOE, Germany) was carried out to determine the purity and phase of TiO_2 nanoparticles.

2.5.3. SEM Analysis

Scanning electron microscopy along energy dispersive spectroscopy (SEM/EDS; Joel JSM 6490A, Japan) was used to analyze the surface/shape/size of TiO_2 nanoparticles and morphology of TiO_2 nanoparticles reinforced PU/CA membranes.

2.5.4. Thermogravimetric Analysis

Thermogravimetric analysis (TGA) of membranes was carried out by using TA instruments SDT Q600 with simultaneous analyzer at a heating rate of 10 °C with nitrogen gas.

2.5.5. Water content

To check the water retention capacity of all membranes, they were soaked in water for 24 hours. Wet weight was calculated. The membranes were then oven dried (12 hours) and their dry weight was calculated. Water swelling studies were conducted by using Eq.1:

$$S = \frac{W_w - W_D}{W_w} \times 100 \qquad \text{(Eq.1)}$$

Where S is swelling ratio of membrane, W_W is wet weight of membrane and W_D is dry weight of membrane.

2.5.6. Contact angle measurement

A sessile drop method-based drop shape analyzer (DSA 30, KRUSS Germany) was used to determine the hydrophilicity of those membranes. I-shaped microsyringe was used to drop the deionized water droplet (5 μL) carefully on the membrane surface. The built-in software determined the contact angle of different membrane samples. The contact angles were measured five times at five different points to obtain their average values to get the correct results.

2.5.7. Tensile strength study

A SHIMADZU AG-X plus series Universal testing machine was used to measure the tensile strength of membranes. The length and width of samples between the jaws were 45mm and 25mm, respectively. The crosshead speed was 3 mm/min, and humidity was maintained at 25±2%. All the measurements were taken roughly at room temperature.

2.5.8. Permeation study

2.5.8.1.Water flux (WF)

A pressure of 1.3 MPa was applied to the membranes for the calculation of water flux by using the following Eq.2 [21]:

$$J_w = {}^{Q}/_{A} \qquad \text{(Eq.2)}$$

Where, J_w is the water flux ($Lm^{-2}h^{-1}$), Q is the volumetric flowrate of permeate whereas, A is the membrane area (m^2).

2.5.8.2.Salt rejection

The percentage salt rejection was calculated with permeate and feed concentration by applying Eq.3:

$$\text{SR}(\%) = \left(1 - {}^{C_p}/_{C_f}\right) \times 100 \qquad \text{(Eq.3)}$$

Where, C_p and C_f are permeate and feed concentrations, respectively.

2.5.9. Testing antibacterial activity of nanoparticles and membranes

To check antibacterial activity, 0.0075g, 0.015g and 0.0225g are consider from five different concentrations of TiO_2 nanoparticles. These nanoparticles were exposed to UV (intensity: 30W, wavelength: 320nm) for 30 minutes and then mixed in liquid nutrient agar (15 mL). Agar was then poured into petri dishes and was allowed to cool. 10^{-3} and 10^{-6} different dilutions of *E. coli* (*Escherichia coli*) and MRSA (Methicillin-Resistant *Staphylococcus Aureus*) were prepared

and spread over the cooled agar plates containing different concentrations of TiO_2 nanoparticles. These plates were then incubated at 37 °C for 24 hours. This step was further investigated by exposing each of these above mentioned TiO_2 nanoparticles concentrations to three different timings of UV exposure and then the impact of time was also compared. Unmodified PC-2 membrane was used as a control sample. At first step, dilutions were prepared. Inoculum of bacteria were added in nutrient broth and were placed in incubator to allow bacteria to grow properly. 1 ml from this broth was added in 9 ml of distilled water to form 10^{-1} dilution. From this dilution, 1 ml was added into another 9ml of distilled water to form 10^{-2} dilution. This process was repeated until 10^{-6} dilutions of each bacterium were obtained.

The enumeration was done by standard plate count given by Eq.4:

$$CFU = \frac{Number\ of\ colonies\ dilution\ factor}{Inoculum\ Size} \quad \text{(Eq.4)}$$

This step was further investigated by exposing each membrane to three different timings of UV exposure and then the impact of time was also compared.

3. Results and discussion

3.1.Structural analysis

The functionalization of TiO_2 nanoparticles was verified by FTIR analysis. The spectrum showed a peak at 1591 cm^{-1} as presented in in Figure 2, which indicated the presence of amine group over the surface of these nanoparticles, while no such peak was observed in non-functionalized nanoparticles. These results are consistent with the literature (Ogi et al., 2002; Jwo et al., 2005; Gupta et al., 2013). These results confirmed the efficient treatment of TiO_2 nanoparticles (Wasim et al., 2017).

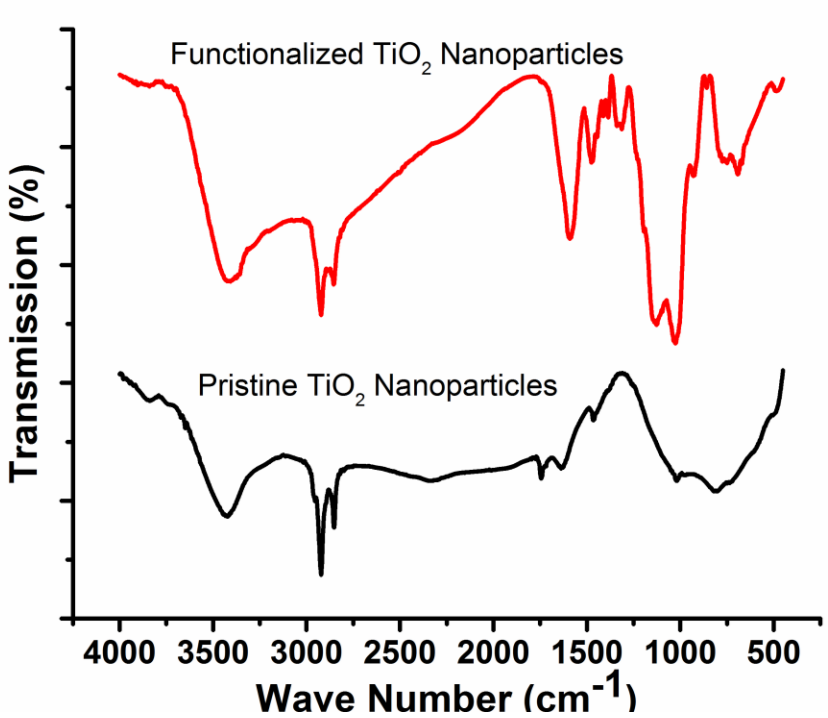

Figure 2. FTIR spectra of pristine and functionalized TiO_2 nanoparticles

In order to characterize different functional groups in membranes, FTIR is used as a key tool. The FTIR spectrum analysis of membranes is shown in Figure 3. The FTIR spectrum of control membrane showed strong peaks at 3650, 2899, 1673, 1593 and 1320. The T-1 membrane showed peaks at 2889,1475,1384,1168 and 100. The T-2 membrane showed peaks at 3640, 2936, 1568, 1442, 1363, 1242, 1164 and 1000. The T-3 membrane showed peaks at 2920, 1477, 1381, 1254 and 1164. The T-4 membrane showed strong peaks at 3520, 2957, 1755, 1469, 1252 and 1093. The T-5 membrane showed peaks at 3510, 2889, 1742, 1465, 1383, 1246 and 1085. When all peaks of membranes were compared in the region of 1400 cm^{-1}, it can be seen that the control membrane had no peaks. This may occur due to the addition of TiO_2 in other membranes (Varshney et al., 2010).

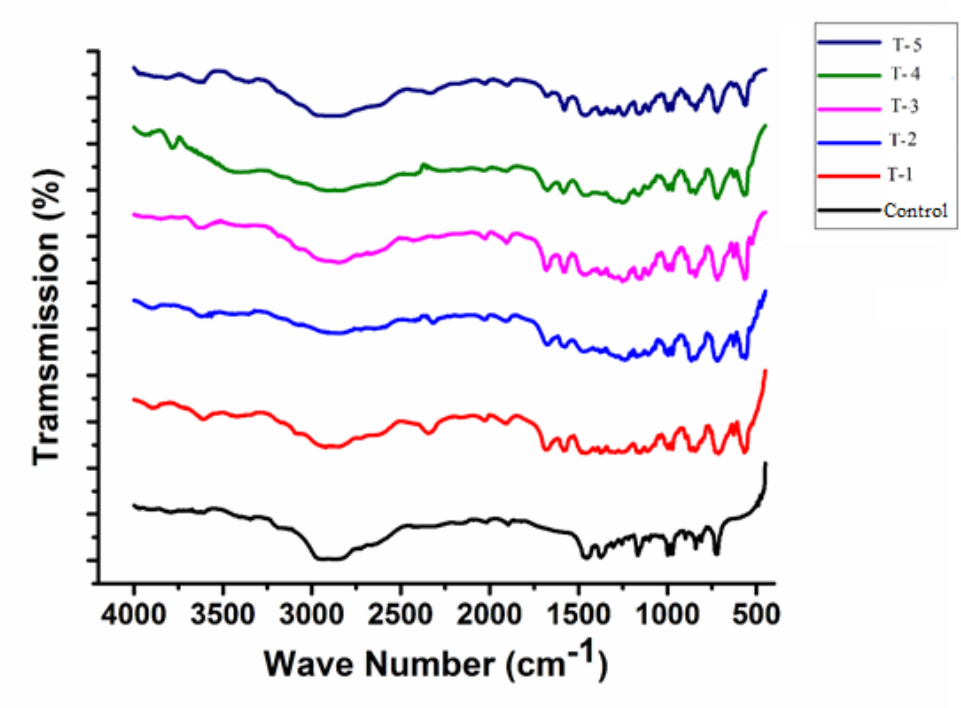

Figure 3. FTIR spectra with increasing concentration of TiO_2 nanoparticles in modified PU/CA membranes

3.2.Crystallinity analysis

Figure 4 presented XRD patterns that were employed to determine the crystal phase of TiO_2 nanoparticles. The crystallite size of nanoparticles obtained in this sample was 41 nm. 91% anatase phase was detected while only 12% brookite was present (Ba-Abbad et al., 2012). The TiO_2 anatase structure was confirmed by the peak at 25° (Thamaphat et al., 2008). The strong diffraction patterns at 25° and 48° also confirmed the anatase structure of these nanoparticles (Theivasanthi and Alagar, 2013). Crystalline structure of particles was confirmed by intensity of XRD peaks while broad diffraction peaks were also indicative of small crystallite size. This XRD pattern agrees with JCPDS card no. 21-1272 (anatase TiO_2) (Ahmad et al., 2017). The XRD peaks at 25.316°, 36.932°, 37.802°, 38.530°, 48.047°, 53.870°, 55.040°, 62.128°, 68.808°, 70.335° and

75.021°can be attributed to the 101, 103, 004, 112, 200, 105, 211, 204, 116, 220 and 215 crystalline structures of anatase synthesized TiO_2 nanoparticles respectively (Gupta et al., 2013).

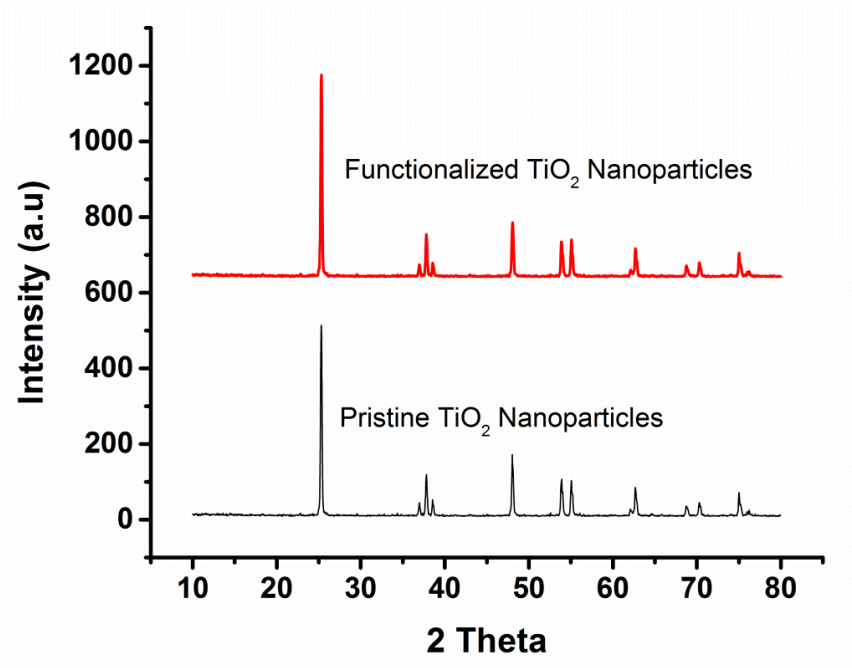

Figure 4. XRD pattern of pristine and functionalized TiO_2 nanoparticles

3.3. Morphological analysis

The morphology of TiO_2 nanoparticles was observed via SEM technique as demonstrated in Figure 5. The nanoparticle size was almost uniform; however, they were in agglomerated form at certain sites. This incident could occur because the nanoparticles were not dispersed in liquid before analysis and were used in powdered form. The average size of nanoparticles obtained was around 64 nm which means they were in nanoscale and can be used further to embed them inside polymer membrane.

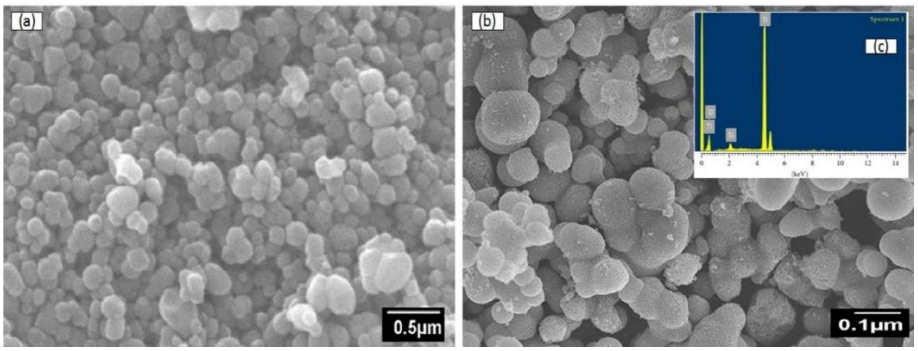

Figure 5. Micrographs (a, b) at various magnifications of TiO_2 nanoparticles along with EDS analysis (c)

The SEM images of all membranes showed difference in pores and overall morphology of membranes when observed from the top and side view is presented in Figure 6. PU/CA control membrane contained uniformly distributed pores. While in other images, with the addition of nanoparticles, fewer pores were observed on the surface of these membranes. It can be noticed that as the concentration of TiO_2 nanoparticles increased, porosity decreased subsequently. Average pore size was measured ranging between 100–500 nm (Mingliang et al., 2011). The higher concentration of nanoparticles in membranes resulted in agglomeration of particles.

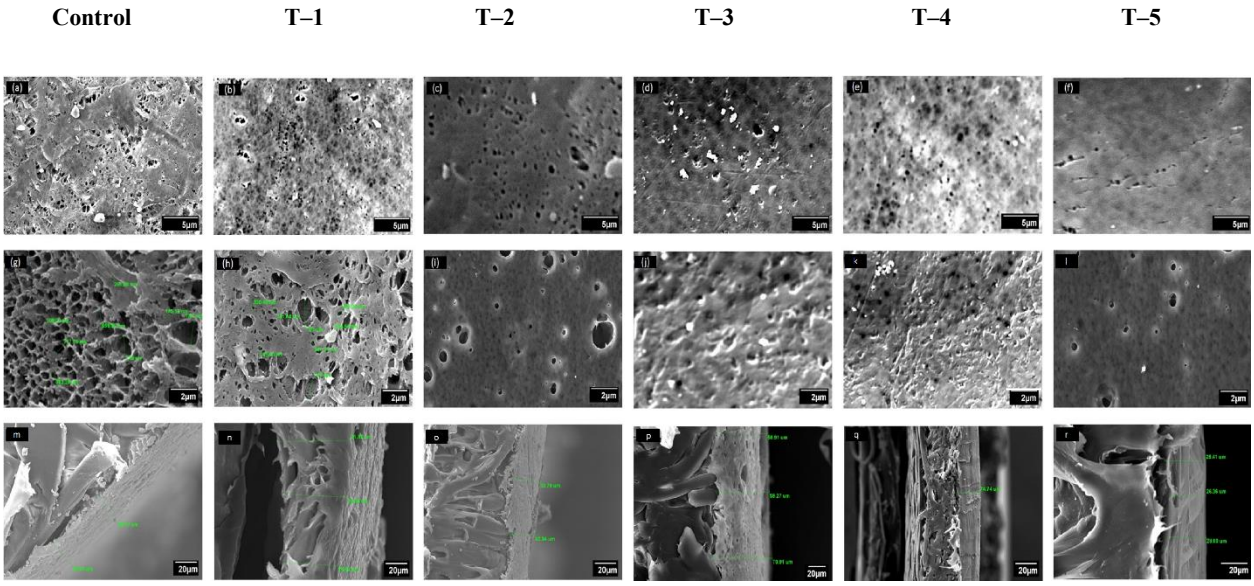

Figure 6. SEM micrographs with increasing concentration of control and TiO_2 modified membranes

The membrane with 0.5% TiO_2 nanoparticles showed higher pore size. This could be attributed to the inclusion of particles in polymeric membranes. During synthesis, these nanoparticles in the casting solution may give more time to non-solvent and solvent solution to be separated which may result higher membrane pore size (Gabriel et al., 2017). The average pore sizes of control, T-1, T-2, T-3, T-4 and T-5 membranes were calculated through SEM and their average values are given in Table 1. The T-5 membrane with 1.5% TiO_2 nanoparticles was not porous and it was not able to calculate average pore size of this membrane. Thickness of the fabricated membranes was found to be approximately similar in case of control membrane and T-1 membrane. However, the membranes with higher concentration of nanoparticles (0.75% and 1.5%) were denser in comparison to other membranes and their thickness was also greater as shown in Table 1. Other differences observed between control and modified membranes were the finger like structure of micro voids. They were elongated across the width of membranes with nanoparticles (Ahmad et al., 2017).

Table 1. Average pore size of control and TiO_2 modified membranes

Membrane Type	**Membrane specs.**	**Average pore size (nm)**
Control	Control (PC-2)	4700-5000
T-1	0.5% TiO_2 + PC-2	1500-2500

T-2	0.75% TiO_2 + PC-2	708-1647
T-3	1.0% TiO_2 + PC-2	600-708
T-4	1.25% TiO_2 + PC-2	550-651
T-5	1.5% TiO_2 + PC-2	300-500

3.4.Thermal gravimetric analysis (TGA)

The membranes were subjected to TGA studies in order to investigate their thermal degradation properties. The thermograms are shown in Figure 7. The major weight loss in T-1 membrane initiated at 290 °C and its degradation continued up to 476 °C, followed by a final decomposition at 492 °C. The major weight loss occurred due to decomposition and splitting of the main polymer chain. The major weight loss in T-2 started at 302 °C and its degradation continued up to 483 °C. The major weight loss in T-3 initiated at 308 °C and its degradation continued up to 495 °C, followed by a final decomposition at 490 °C. The major weight loss in T-4 started at 325 °C and its degradation continued up to 505°C. The major weight loss in T-5 started at 345 °C and its degradation continued up to 530°C. These behaviors are due to the addition of TiO_2 nanoparticles.

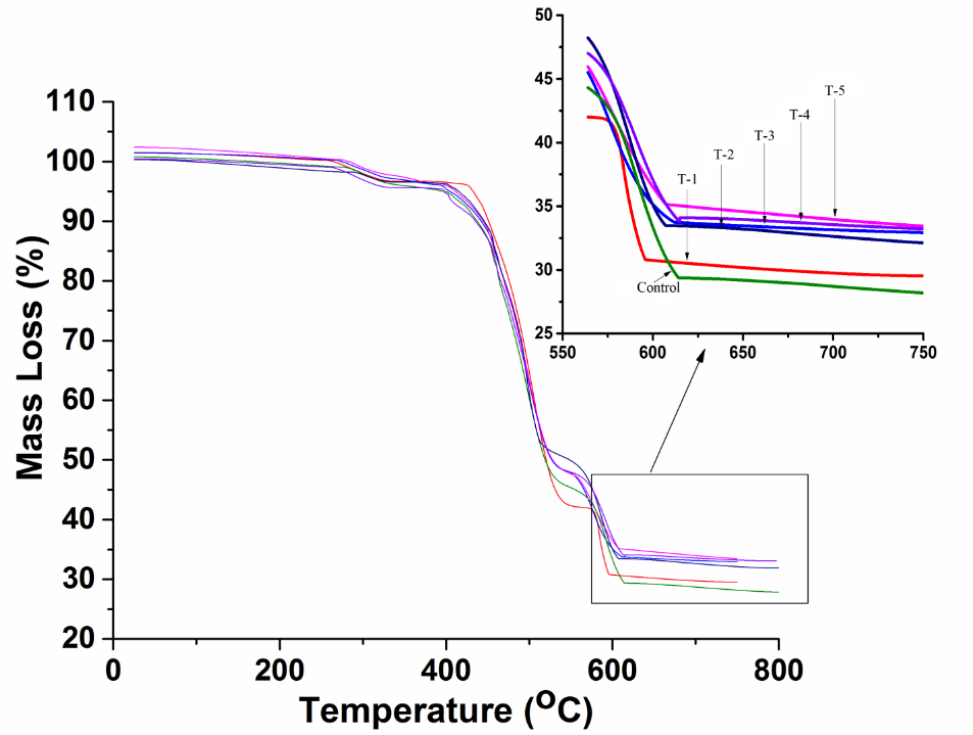

Figure 7. Thermograms of control and TiO_2 modified membranes

The TGA studies results are summarized in the Table 2. It was observed that in membrane with highest concentration of nanoparticles (T-5), the stability is highest (305°C). This means by increasing the concentration of nanoparticles, the polymer membrane became more stable. However, prominent differences were observed in T-2 and T-5.

3.5. Water retention by membranes

Figure 8 shows the water retention profile of control and TiO_2 modified membranes. The lowest % of water retention was showed by T-3. Maximum water retention was observed in the T-5 membrane (Figure 7) that has the maximum percentage of incorporated nanoparticles. This indicates that addition of TiO_2 nanoparticles enhanced the hydrophilicity of the membrane. The hydroxyl groups present on the surface of TiO_2 nanoparticles have high surface area that is responsible for its high hydrophilicity. As the hydroxyl content of the membrane increased,

hydrophilicity of the membrane also increased significantly (Mingliang et al., 2011; Munnawar et al., 2017).

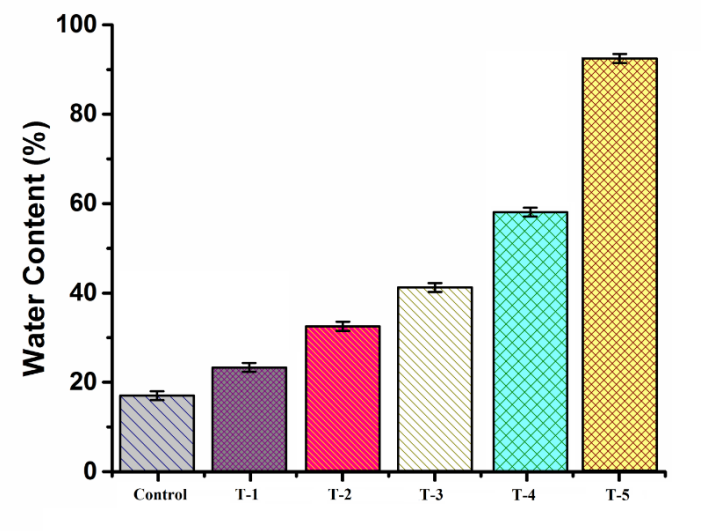

Figure 8. Water retention profile of control and TiO_2 modified membranes

3.6. Contact angle measurements

Contact angle measurements were conducted for measuring the hydrophilicity of membranes. Increase in hydrophilicity with increasing concentration of TiO_2 nanoparticles was pragmatic as seen in Figure 9. This may occur due to incorporation of hydrophilic TiO_2 nanoparticles in the membrane. Thus, a visible decrease in contact angle values was recorded with increasing concentration of nanoparticles as mentioned in Table 4 (Mingliang et al., 2011; Rahimpour et al., 2011).

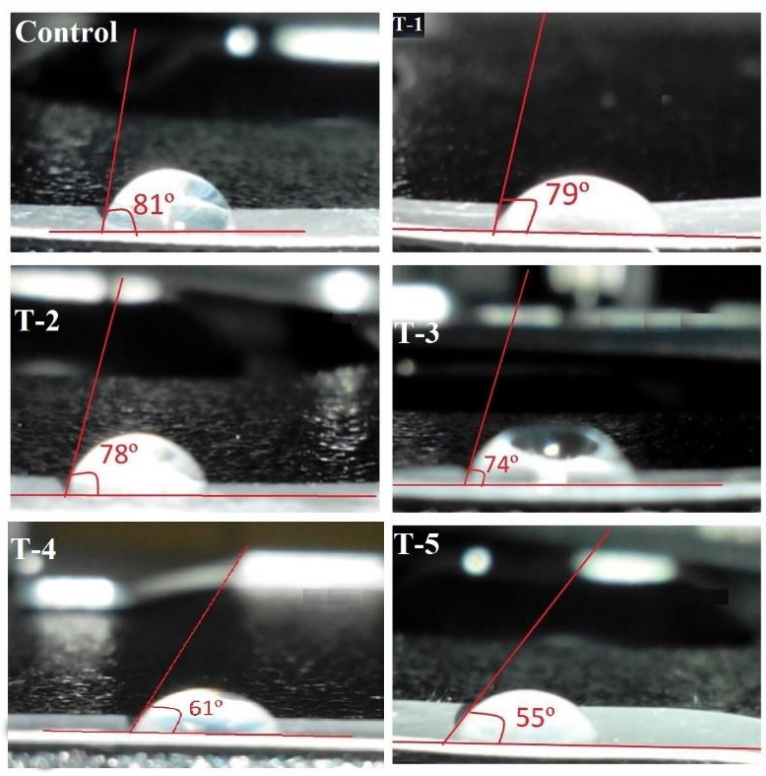

Figure 9. Contact angle of control and TiO_2 modified membranes

3.7.Mechanical testing

The mechanical properties were characterized to analyze the effect of nanoparticles on the strength of membranes shown in Figure 10. The values of tensile strength and elongation of all membranes including control sample are summarized in Table 2. The mechanical testing revealed that as the concentration of nanoparticles increased, their resulting tensile strength and elongation at break also increased. The T-1, T-2 and T-3 membranes showed an upsurge in their mechanical strength and this trend continued until T-5 membrane, which showed maximum strength.

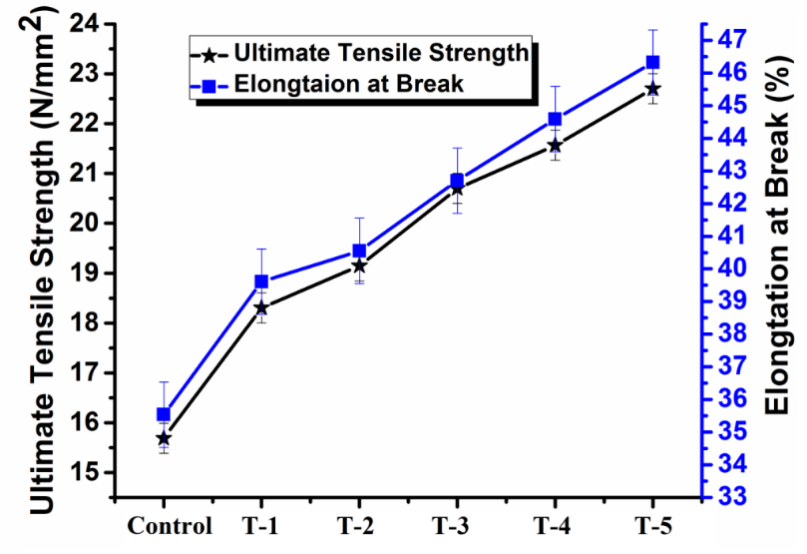

Figure 10. UTS and elongation at break of control and TiO_2 modified membranes

Table 2. Mechanical strength and thermal stability of control and TiO_2 modified membranes

Membrane	Tensile strength (N/mm^2)	Elongation at break (%)	TGA(°C)	
			Onset Temperature (^OC)	Offset Temperature (^OC)
Control	15.68±0.01	35.9±0.25	280	465
T-1	18.45±0.01	39.88±0.1	290	476
T-2	19.55±0.01	40.55±0.1	302	483
T-3	20.50±0.01	42.75±0.1	308	495
T-4	22.10±0.01	44.65±0.3	325	505

T-5	23.56±0.01	46.45±0.1	345	530

Membranes exhibited good mechanical strength supporting good compatibility of nanoparticles with polymer matrix. This increase in mechanical strength occurred due to the incorporation of nanoparticles that were responsible for creating higher interconnections between the polymeric chains (Iqbal et al., 2013).

3.8.Permeation analysis

The permeation results for PC-1, PC-2, PC-3 and PC-4 membranes have been shown in Table 3. PC-2 was selected for the modification with Titania nanoparticles because of its optimum values of flux and salt rejection. In PC-1, Flux is high, but rejection is low enough, in PC-3 and PC-4 the values for flux are too low.

The permeation properties of control and modified membranes are detailed in Table 4. Indigenously fabricated permeation setup was used for this experiment as shown in Figure. 1. The flux and salt rejection properties showed increasing trend as observed in Table 4.

Table 3. Permeation properties of PC-1, PC-2, PC-3 and PC-4 membranes.

Membrane Type	**Flux (L/h.m^2)**	**Salt Rejection (%)**
PC–1 (PU: 90%, CA: 10%)	13.50	85±0.5
PC–2 (PU: 80%, CA: 20%)	10.98	90±0.5
PC–3 (PU: 80%, CA: 30%)	7.96	94±0.5

PC–4 (PU: 60%, CA: 40%)	5.84	95±0.5

The control membrane exhibited the minimum value of salt rejection and maximum flux due to porous structure of the membranes. The modified membranes showed the increasing trend for both salt rejection and flux. The water flux was increased by increasing the concentration of nanoparticles in the membrane due to hydrophilic nature of TiO_2. The salt rejection showed the increasing behavior by increasing the concentration of nanoparticles. This increase may occur because of decrease in pore size of these membranes. It was due to the structural changes in the modified membranes. Other characterization techniques e.g. water content and contact angle also proved that the addition of nanoparticles increased the hydrophilicity of the membrane (Arsuaga et al., 2013; Ahmad et al., 2017).

Table 4. Various characteristics of control and TiO_2 modified membranes

Membrane	**Membrane Composition**	**Contact Angle**	**Salt Rejection (%)**	**Flux (L/h.m^2)**
Control	PC–2 (PU: 80%, CA: 20%)	81º ±0.1	90±0.5	10.98
T-1	PC-2+0.25% TiO_2	79º±0.1	93±0.5	11.02
T-2	PC-2+0.5% TiO_2	78º±0.1	96±0.5	12.40
T-3	PC-2+0.75% TiO_2	74º±0.1	97±0.5	12.98

T-4	PC-2+1.00% TiO_2	61º±0.1	97.5±0.5	13.95
T-5	PC-2+1.25% TiO_2	55º±0.1	98±0.5	16.76

3.9.Antibacterial activity test

The activity of nanoparticles against MRSA and *E. coli* was analyzed by taking three different concentrations of nanoparticles i.e., 0.5 wt%, 1.0 wt% and 1.5 wt%. Results showed that the antibacterial activity increased by increasing concentration of nanoparticles. It can be seen in Figure 11 that the plate with 0.5 wt% of TiO_2 nanoparticles showed maximum growth of bacteria. Almost whole agar plate was covered with bacterial growth as shown in Figure 11.

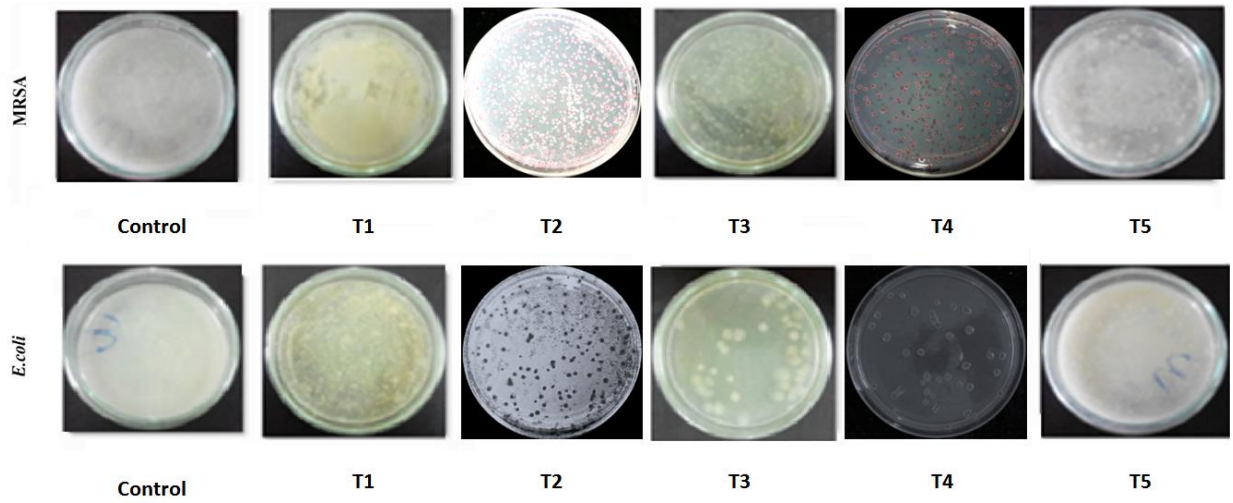

Figure 11. Images of bacterial activity against *MRSA* and *E. coli*

While this trend of bacterial growth was decreased in other two agar plates as the concentration of nanoparticles was increased, the plate with maximum concentration of nanoparticles showed minimum bacterial growth which is also consistent with another study (Bashir et al., 2018).

The fabricated membranes with TiO_2 nanoparticles exemplified the superlative properties as observed in various characterizations used in this study. The antibacterial activity of fabricated

membranes was proven by the decrease in bacterial colonies on the agar plates, due to photocatalytic bactericidal effect of TiO_2 nanoparticles. The maximum inhibition was observed in membrane with maximum nanoparticles when compared with other membranes, which are observed by the values of colony forming unit count (cfu) as shown in Figure 12.

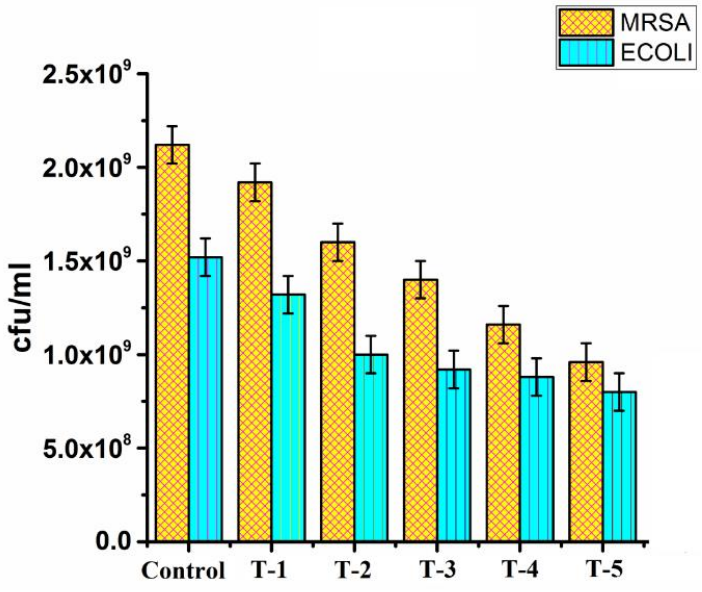

Figure 12. Antibacterial activity of control and TiO_2 nanoparticles modified membranes

Effect of time variation of UV exposure was also investigated, and maximum inhibition was seen when membranes were exposed for 90 min as depicted in Figure 13. The duration of UV exposure affected the antibacterial activity of membrane due to increased exposure of nanoparticles to UV radiations. Titania (TiO_2)-based nanocomposites subjected to light excitation are remarkably effective in eliciting microbial death. The photocatalytic action triggers in UV which may decreased expression of a large array of genes/proteins specific for regulatory, signaling and growth functions in parallel with subsequent selective effects on ion homeostasis, coenzyme-independent respiration and cell wall structure (Kubacka et al., 2014).

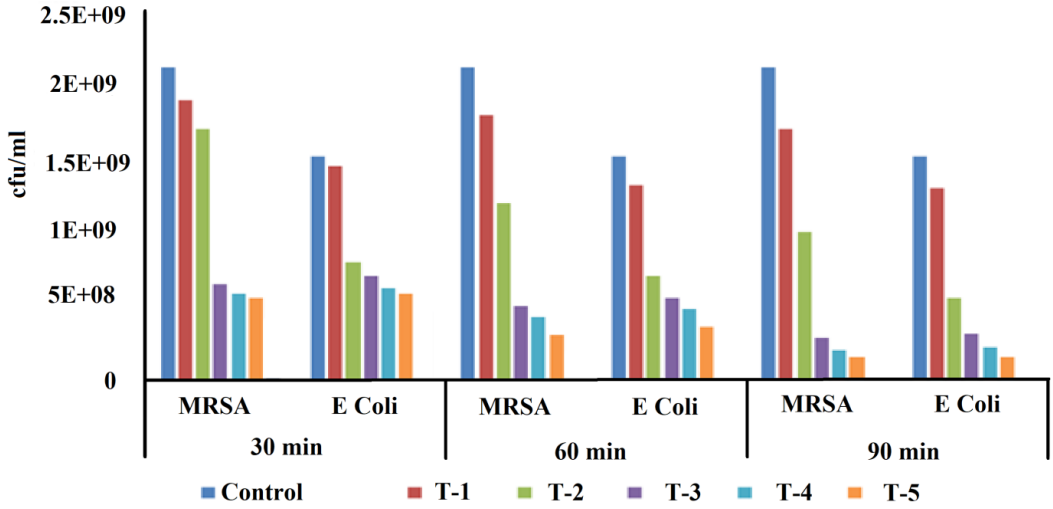

Figure 13. Statistical analysis of bacterial effect in the presence of UV for TiO_2 nanoparticles modified PU/CA membranes

The evidence from the designed modified membranes that TiO_2 photocatalysis causes rapid cell inactivation at regulatory and other signaling levels. The coenzyme independent respiratory chains were also decreased because of this phenomenon. It also decreased assimilation and transport of phosphorus and iron ions. This decreased the capacity for synthesis as well as degradation of Fe-S clusters. These factors collectively contribute in the cell wall modification and high biocidal performance of TiO_2 nanoparticles as also mentioned by Arribas *et al.(Barbas Arribas and Rojo Blanco, 2015)*. Hence, it was proved from this analysis that these TiO_2 modified membranes exhibit substantial antibacterial properties. The antibacterial performance of these membranes directly depended on the concentration of nanoparticles and their subsequent UV exposure.

4. Conclusions

The inhibition of *E. coli* and *MRSA* by TiO_2 nanoparticles was confirmed. Functionalized TiO_2 nanoparticles incorporated mixed matrix membranes were successfully synthesized for water treatment. These antibacterial membranes showed good inhibition under UV irradiation. Their antibacterial activity increased by increasing the duration of UV exposure. The characterization of nanoparticles and membranes showed good results. Membrane properties such as hydrophilicity, thermal stability, water flux and salt rejection and mechanical strength were enhanced by increasing the concentration of TiO_2 nanoparticles.

Acknowledgement

I would like to thank Taif University Researchers Supporting Project number (TURSP-2020/260), Taif University, Taif, Saudi Arabia.

Conflict of Interest

The authors declare no conflicts of interest.

References

Abdullah, N., Yusof, N., Lau, W., Jaafar, J., Ismail, A., 2019. Recent trends of heavy metal removal from water/wastewater by membrane technologies. Journal of Industrial and Engineering Chemistry 76, 17-38.

Ahmad, A., Jamshaid, F., Adrees, M., Iqbal, S.S., Sabir, A., Riaz, T., Zaheer, H., Islam, A., Jamil, T., 2017. Novel Polyurethane/Polyvinyl chloride-co-vinyl acetate crosslinked membrane for reverse osmosis (RO). Desalination 420, 136-144.

Ahmad, A., Jamshed, F., Riaz, T., Waheed, S., Sabir, A., AlAnezi, A.A., Adrees, M., Jamil, T., 2016. Self-sterilized composite membranes of cellulose acetate/polyethylene glycol for water desalination. Carbohydrate polymers 149, 207-216.

Ahmad, A., Waheed, S., Khan, S.M., Shafiq, M., Farooq, M., Sanaullah, K., Jamil, T., 2015. Effect of silica on the properties of cellulose acetate/polyethylene glycol membranes for reverse osmosis. Desalination 355, 1-10.

Ahmadiannamini, P., Eswaranandam, S., Wickramasinghe, R., Qian, X., 2017. Mixed-matrix membranes for efficient ammonium removal from wastewaters. Journal of Membrane Science 526, 147-155.

Arsuaga, J.M., Sotto, A., del Rosario, G., Martínez, A., Molina, S., Teli, S.B., de Abajo, J., 2013. Influence of the type, size, and distribution of metal oxide particles on the properties of nanocomposite ultrafiltration membranes. Journal of membrane science 428, 131-141.

Azizullah, A., Khattak, M.N.K., Richter, P., Häder, D.-P., 2011. Water pollution in Pakistan and its impact on public health—a review. Environment international 37, 479-497.

Ba-Abbad, M.M., Kadhum, A.A.H., Mohamad, A.B., Takriff, M.S., Sopian, K., 2012. Synthesis and catalytic activity of TiO2 nanoparticles for photochemical oxidation of concentrated chlorophenols under direct solar radiation. Int. J. Electrochem. Sci 7, 4871-4888.

Bagheri, S., Shameli, K., Abd Hamid, S.B., 2013. Synthesis and characterization of anatase titanium dioxide nanoparticles using egg white solution via Sol-Gel method. Journal of Chemistry 2013.

Barbas Arribas, C., Rojo Blanco, D., 2015. Understanding the antimicrobial mechanism of TiO2-based nanocomposite films in a pathogenic Bacterium/David Rojo...[et al.].

Bashir, A., Jabeen, S., Gull, N., Islam, A., Sultan, M., Ghaffar, A., Khan, S.M., Iqbal, S.S., Jamil, T., 2018. Co-concentration effect of silane with natural extract on biodegradable polymeric films for food packaging. International journal of biological macromolecules 106, 351-359.

Blake, D.M., Maness, P.-C., Huang, Z., Wolfrum, E.J., Huang, J., Jacoby, W.A., 1999. Application of the photocatalytic chemistry of titanium dioxide to disinfection and the killing of cancer cells. Separation and purification methods 28, 1-50.

Chen, Haisheng, Shengyang Zheng, Lijun Meng, Gang Chen, Xubiao Luo, and Manhong Huang. "Comparison of novel functionalized nanofiber forward osmosis membranes for application in antibacterial activity and TRGs rejection." Journal of hazardous materials 392 (2020): 122250.

Ekey, K., 2013. Tick Toxic: the failure to clean up TSCA poisons public health and threatens chemical innovation. Wm. & Mary Envtl. L. & Pol'y Rev. 38, 169.

Gabriel, L.P., Rodrigues, A.A., Macedo, M., Jardini, A.L., Maciel Filho, R., 2017. Electrospun polyurethane membranes for Tissue Engineering applications. Materials Science and Engineering: C 72, 113-117.

Geise, G.M., Lee, H.S., Miller, D.J., Freeman, B.D., McGrath, J.E., Paul, D.R., 2010. Water purification by membranes: the role of polymer science. Journal of Polymer Science Part B: Polymer Physics 48, 1685-1718.

Gupta, K., Singh, R., Pandey, A., Pandey, A., 2013. Photocatalytic antibacterial performance of TiO2 and Ag-doped TiO2 against S. aureus. P. aeruginosa and E. coli. Beilstein journal of nanotechnology 4, 345-351.

Halder, P., Hossain, N., Pramanik, B.K., Bhuiyan, M.A., 2020. Engineered topographies and hydrodynamics in relation to biofouling control—a review. Environmental Science and Pollution Research.

Hossain, N., Mahmud, L., 2019. Experimental Investigation of Water Quality and Inorganic Solids in Malaysian Urban Lake, Taman Tasik Medan Idaman. Lakes & Reservoirs: Science, Policy and Management for Sustainable Use 24, 107-114.

Ibrahim, S.M., Nagasawa, H., Kanezashi, M., Tsuru, T., 2017. Organosilica bis (triethoxysilyl) ethane (BTESE) membranes for gas permeation (GS) and reverse osmosis (RO): The effect of preparation conditions on structure, and the correlation between gas and liquid permeation properties. Journal of Membrane Science 526, 242-251.

Iqbal, N., Ahmad, N.M., Sagar, S., Iqbal, F., Tareen, M.H., Khan, T.A., Mehfooz, S., Khan, M.B., Jameel, T., 2013. Development of kevlar-supported novel polypropylene membranes: Effect of the concentration of the nucleating agent on the properties and performance. Journal of Applied Polymer Science 130, 2821-2831.

Jacangelo, J.G., Trussell, R.R., Watson, M., 1997. Role of membrane technology in drinking water treatment in the United States. Desalination 113, 119-127.

Jwo, C.S., Teng, T.P., Chang, H., Tsung, T.T., Liao, C.Y., Lin, C.H., 2005. Preparation and UV characterization of TiO2 nanoparticles synthesized by SANSS. Reviews on Advanced Materials Science 10, 283-288.

Kubacka et al., 2014 A. Kubacka, M.S. Diez, D. Rojo, R. Bargiela, S. Ciordia, I. Zapico, J.P. Albar, C. Barbas, V. dos Santos, M. Fernandez-Garcia, M. Ferrer. Understanding the antimicrobial mechanism of TiO2-based nanocomposite films in a pathogenic bacterium. Sci. Rep., 4 (2014), p. 9

Kumar, R., Isloor, A.M., Ismail, A., Rashid, S.A., Al Ahmed, A., 2013. Permeation, antifouling and desalination performance of TiO2 nanotube incorporated PSf/CS blend membranes. Desalination 316, 76-84.

Kwak, S.-Y., Kim, S.H., Kim, S.S., 2001. Hybrid organic/inorganic reverse osmosis (RO) membrane for bactericidal anti-fouling. 1. Preparation and characterization of TiO2 nanoparticle self-assembled aromatic polyamide thin-film-composite (TFC) membrane. Environmental science & technology 35, 2388-2394.

Li, J.B., Zhu, J.W., Zheng, M.S., 2007. Morphologies and properties of poly (phthalazinone ether sulfone ketone) matrix ultrafiltration membranes with entrapped TiO2 nanoparticles. Journal of applied polymer science 103, 3623-3629.

Majid, Abdul, Salah Ud-Din Khan, Sajjad Haider, and J. J. Zhu. "Effects of thermal annealing on structural and magnetic properties of Mn ions implanted AlInN/GaN films." Journal of Magnetism and Magnetic Materials 469 (2019): 618-622.

Majid, Abdul, Muhammad Tanveer, Usman Ali Rana, Salah Ud-Din Khan, and Saadia Kousar. "Facile synthesis of Mn-doped CdTe nanoparticles: structural and magnetic properties." Journal of Superconductivity and Novel Magnetism 29, no. 10 (2016): 2615-2619.

Mingliang, L., Qingzhi, W., Jialin, L., Hongjian, L., Zilong, J., 2011. Fabrication of SPES/nano-TiO2 composite ultrafiltration membrane and its anti-fouling mechanism. Chinese Journal of Chemical Engineering 19, 45-51.

Munnawar, I., Iqbal, S.S., Anwar, M.N., Batool, M., Tariq, S., Faitma, N., Khan, A.L., Khan, A.U., Nazar, U., Jamil, T., 2017. Synergistic effect of Chitosan-Zinc Oxide Hybrid Nanoparticles on antibiofouling and water disinfection of mixed matrix polyethersulfone nanocomposite membranes. Carbohydrate polymers 175, 661-670.

Nagaraju, D., Sastri, J., 1999. Confirmed faecal pollution to bore well waters of Mysore city. Environmental Geology 38, 322-326.

Ogi, H., Hirao, M., Shimoyama, M., 2002. Activation of TiO2 photocatalyst by single-bubble sonoluminescence for water treatment. Ultrasonics 40, 649-650.

Organization, W.H., 1993. Guidelines for drinking-water quality. World Health Organization.

Rahimpour, A., Jahanshahi, M., Mollahosseini, A., Rajaeian, B., 2012. Structural and performance properties of UV-assisted TiO2 deposited nano-composite PVDF/SPES membranes. Desalination 285, 31-38.

Rahimpour, A., Jahanshahi, M., Rajaeian, B., Rahimnejad, M., 2011. TiO2 entrapped nano-composite PVDF/SPES membranes: Preparation, characterization, antifouling and antibacterial properties. Desalination 278, 343-353.

Shannon, M.A., Bohn, P.W., Elimelech, M., Georgiadis, J.G., Marinas, B.J., Mayes, A.M., 2010. Science and technology for water purification in the coming decades. Nanoscience and technology: a collection of reviews from nature Journals, 337-346.

Shar, A.H., Kazi, Y.F., Soomro, I., Zardari, M., 2009. Bacteriological quality of drinking water of Sukkur City. Pakistan Journal of Medical Research 48, 88-90.

Thamaphat, K., Limsuwan, P., Ngotawornchai, B., 2008. Phase characterization of TiO2 powder by XRD and TEM. Agriculture and Natural Resources 42, 357-361.

Theivasanthi, T., Alagar, M., 2013. Titanium dioxide (TiO2) nanoparticles XRD analyses: an insight. arXiv preprint arXiv:1307.1091.

Varshney, R., Bhadauria, S., Gaur, M., 2010. Biogenic synthesis of silver nanocubes and nanorods using sundried Stevia rebaudiana leaves. Adv. Mat. Lett 1, 232-237.

Vassolo, S., Döll, P., 2005. Global-scale gridded estimates of thermoelectric power and manufacturing water use. Water Resources Research 41.

Wasim, M., Sagar, S., Sabir, A., Shafiq, M., Jamil, T., 2017. Decoration of open pore network in Polyvinylidene fluoride/MWCNTs with chitosan for the removal of reactive orange 16 dye. Carbohydrate polymers 174, 474-483.

Water, S., Organization, W.H., 2004. Water, sanitation and hygiene links to health: facts and figures.

Yan, H., Wang, X., Yao, M., Yao, X., 2013. Band structure design of semiconductors for enhanced photocatalytic activity: The case of TiO2. Progress in Natural Science: Materials International 23, 402-407.

Yuzer, Burak, Muhammed Iberia Aydın, Ahmet Hilmi Con, Hatice Inan, Safiye Can, Huseyin Selcuk, and Yassine Kadmi. "Photocatalytic, self-cleaning and antibacterial properties of Cu (II) doped TiO2." Journal of Environmental Management 302 (2022): 114023.